Journal of Biomechanics 150 (2023) 111510

Contents lists available at ScienceDirect

Journal of Biomechanics

journal homepage: www.elsevier.com/locate/jbiomech

Optimization of patient positioning for improved healing after corneal transplantation

V. Garcia Bennett [a], M. Alberti [b], M. Quadrio [a], J.O. Pralits [c,*]

[a] Department of Aerospace Science and Technologies, Politecnico di Milano, Milano, Italy
[b] Department of Ophthalmology, Rigshospitalet, Glostrup, Denmark
[c] Department of Civil, Chemical and Environmental Engineering, University of Genova, Genova, Italy

ARTICLE INFO

Keywords:
Endothelial keratoplasty
Intraocular gas
Patient positioning
Computational fluid dynamics
DMEK

ABSTRACT

Corneal transplantation is the only solution which avoids loss of vision, when endothelial cells are dramatically lost. The surgery involves injecting gas into the anterior chamber of the eye, to create a bubble that pushes onto the donor cornea (graft), achieving sutureless adherence to the host cornea. During the postoperative period, patient positioning affects the bubble. To improve healing, we study the shape of the gas-bubble interface throughout the postoperative period, by numerically solving the equations of fluid motion. Patient-specific anterior chambers (ACs) of variable anterior chamber depths (ACD) are considered, for either phakic (with natural lens) and pseudophakic (with artificial lens) eyes. For each AC, gas-graft coverage is computed for different gas fill and patient positioning. The results show that the influence of positioning is negligible, regardless of gas filling, as long as the ACD is small. However, when the ACD value increases, patient positioning becomes important, especially for pseudophakic ACs. The difference between best and worst patient positioning over time, for each AC, is negligible for small ACD but significant for larger ACD, especially for pseudophakic eyes, where guidelines for optimal positioning become essential. Finally, mapping of the bubble position highlights the importance of patient positioning for an even gas-graft coverage.

1. Introduction

Corneal endothelial dysfunction of the human eye occurs when corneal endothelial cells are dramatically lost, and eventually results in vision loss. Corneal transplantation is presently the only viable solution. For patients with an endothelial disease such as Fuch's endothelial dystrophy, endothelial keratoplasty (EK) is currently the mainstay of definitive treatment and path for restoration of vision (Stuart et al., 2018; Melles et al., 2006; Deng et al., 2018). The number of people estimated to have the Fuch's subtype of endothelial dystrophy worldwide (>30 years) will increase from 300 million in 2020 to 415 million in 2050 (Aiello et al., 2022). In EK only a portion of the posterior cornea is removed and replaced by a ≈40 μm thick and ≈ 8.5 mm diameter donor cornea (graft). In techniques such as Descemet's membrane endothelial keratoplasty (DMEK) a gas, such as air or SF6, is injected into the anterior chamber (AC) to create a bubble that pushes onto the graft, ensuring sutureless adherence of the donor graft to the host cornea (Price et al., 2018) during healing. The maximal gas fill is patient dependent, however, up to approximately 80% is possible without an inferior iridotomy.

Studies (Tourtas et al., 2014), evaluated on 200 patients, have shown that gas left in the anterior chamber after surgery is completely absorbed within 48 to 72 h and that 90% of graft detachments are identified within this period.

Defining graft detachment as significant if the radial extent of the non adherent surface is at least 1 mm (on a 8 mm graft), a study (Tourtas et al., 2014) of 51 patients showed that the graft detachment rate 4 days after surgery was between 33.3% and 78.3% depending on the difference between the descemetorhexis and graft diameters. Note that in this study all patients were asked to stay 48 h in supine position after surgery.

Studies suggest that a larger bubble helps preventing graft detachment and the need for re-bubbling procedures (Ćirković et al., 2016; Leon et al., 2018), whereas gas overfill leads to complications such as pupillary block (Gonzalez et al., 2016) and raises concerns of possible endothelial toxicity (Kopsachilis et al., 2013; Landry et al., 2011). The optimal gas fill after DMEK is unknown, and a lack of knowledge of gas behavior in the anterior chamber hinders optimal surgical results.

* Corresponding author.
E-mail addresses: v.garciabennett@gmail.com (V.G. Bennett), markalberti@gmail.com (M. Alberti), maurizio.quadrio@polimi.it (M. Quadrio), jan.pralits@unige.it (J.O. Pralits).

https://doi.org/10.1016/j.jbiomech.2023.111510
Accepted 17 February 2023
Available online 24 February 2023

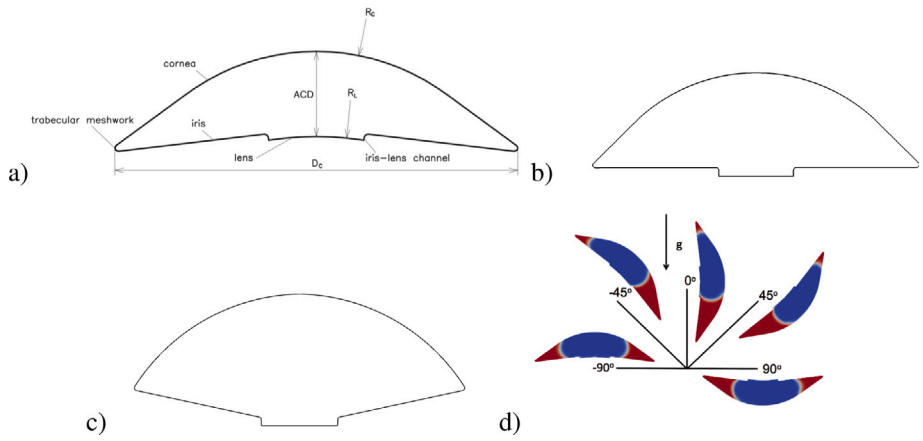

Fig. 1. Symmetry plane of the anterior chamber geometries; (a) phakic eye including definition of dimensions; (b) pseudophakic eye ACD = 3.45 and ACD = 4.35 mm (flat iris) (c) pseudophakic eye ACD = 5.00 mm. See Table 1 for abbreviations and parameter values. (d) Definition of gaze angle, ψ. −90° supine position; 0° horizontal gaze; 90° prone position.

Numerical analysis, as a support to investigate bio-mechanical problems, is nowadays common practice in a large number of applications. In the case of biofluid dynamics of the human eye, the methods ranges from semi analytical, to simulations of the fluid flow in one, two, and three dimensions: a few examples include (Isakova et al., 2017; Repetto et al., 2015; Isakova et al., 2014; Davvalo Khongar et al., 2019). Recent numerical experiments (Pralits et al., 2019) have indicated that gas fill is the most important variable for ensuring graft coverage in phakic eyes, i.e. eyes with a natural lens; both gas fill and patient positioning become important to ensure gas-graft coverage in pseudophakic eyes, i.e. eyes with artificial lens, especially as the anterior chamber depth (ACD) increases. However, these results do not account for the effect of changes in patient positioning during the postoperative period, and for the diminishing size of the gas bubble as time progresses.

In an effort to maximize graft coverage by intraocular gas, the aim of this paper is to provide a more complete understanding of gas coverage of the endothelial graft throughout the postoperative period. Moreover, the analysis also allows to examine relationships between one-dimensional bubble height (which is the surgeons' common measure), two-dimensional gas-graft contact area, and three-dimensional gas volume. To this end, a numerical study of gas fill in model and patient-specific anterior chambers is carried out, including the DMEK graft. The true three-dimensional shape of the gas bubble is computed for both phakic and pseudophakic ACs, accounting for the properties of air and aqueous humor (AH). For each geometry the gas coverage on the graft is computed for different values of the gas fill and patient positioning. Moreover, a technique to evaluate the position is introduced which provides not only the gas coverage percentage, but also the spatial details of the coverage. This is particularly important when studying the causes of graft detachment (Price et al., 2018). Different cases of patient positioning over time are considered, and the difference between "best-case" and "worst-case" scenarios is quantified.

2. Materials and methods

The anterior chamber (AC) of the phakic and pseudophakic eye is modeled as a rigid and idealized geometry (Pralits et al., 2019), although in reality it is flexible and vascularized. Three values of the anterior chamber depth (ACD) are studied for both phakic and pseudophakic cases: the minimum, average and maximum. These values are taken from a Fuch's endothelial dystrophy patient population eligible for endothelial keratoplasty procedures involving air/gas in the AC (ClinicalTrials.gov identifier: NCT03407755). The geometrical characteristics of the ACs are given in Fig. 1 and Table 1. All phakic cases are based on the geometry shown in Fig. 1a while the pseudophakic cases are based on two different geometries; the two smaller ACD values are modeled with a flat iris, while the larger one (ACD = 5 mm) is given a concave iris which compares better with large gas-filled ACDs. Clinical aspects of this study involving patients are in accordance with the tenets of the Declaration of Helsinki.

2.1. Description of the mathematical model

The equilibrium position of the fluid–gas interface was computed numerically, following the procedure described in Pralits et al. (2019), by solving the incompressible, isothermal Navier–Stokes equations for two immiscible fluids. The equilibrium position is defined as the shape of the interface, between the fluid and gas, which is obtained after a time long enough such that the fluid and gas are both at rest. The fluid–gas interface is tracked using the Volume of Fluid method (OpenFOAM, 2022). Table 1 shows the values of the fluid properties used. In particular, clinical trials have been conducted to experimentally obtain the contact angle at the cornea, α_{cornea}. Previous observations (Alberti, 2018) found a contact angle based on patient measurements with anterior segment optical coherence tomography (OCT) to be: $\alpha_{\text{cornea}} = 16.8° \pm 3.1°$. For simplicity $\alpha_{\text{cornea}} = 17°$ is used in all simulations. To date there are no clinical trials which have determined the contact angle at the iris, α_{iris}. Here we assumed that it is equal to the one at the lens, α_{lens} (Miyake et al., 1994), $\alpha_{\text{iris}} = \alpha_{\text{lens}} = 24.0°$. A careful study has shown that this assumption does not alter the final results of our procedure. The shape and position of the gas bubble in contact with the cornea are obtained by solving the equations of fluid motion for different values of gas fill and patient positions. Prior to the study the numerical model was validated. The volume of fluids approach was validated as in Isakova et al. (2017) by comparison with an analytical solution in a spherical domain. Here, unstructured meshes consisting of tetragonal and hexahedral volumes are produced using the snappyHexMesh tool by OpenFOAM. We used, on average, 1.2 million volumes to perform three-dimensional simulations and run the code in parallel on a 36-processor computer at the high-performance computing center CINECA (Bologna, Italy). Before the simulations, careful mesh-independence tests have been made, similar to what was done in Pralits et al. (2019).

2.2. Parameters and observables

The graft diameter is 8.5 mm: a frequently used size which aims to balance total endothelial cell count and intra-operative graft handling. The percentage of the graft covered by gas is analyzed as a function

Table 1
Parameter abbreviations and values for the three phakic and pseudophakic AC geometries, and fluid properties.

Parameter	Abbreviation	Value
Geometrical characteristics of the phakic ACs		
AC volume	V_{AC}	0.105/0.170/0.271 [mL]
AC diameter	D_{AC}	12.5/12.5/12.5 [mm]
AC depth (Alberti, 2018)	ACD	1.79/2.65/3.68 [mm]
Posterior cornea minimum radius of curvature (Von Helmholtz, 1909)	R_C	6.8/6.8/6.8 [mm]
Radius of curvature of the natural lens	R_L	10.0/10.0/10.0 [mm]
Height of the iris–lens channel	–	0.10/0.10/0.10 [mm]
Angle between cornea and iris	–	16.2/28.6/47.9 [deg]
Geometrical characteristics of the pseudophakic ACs		
AC volume	V_{AC}	0.219/0.279/0.309 [mL]
AC diameter	D_{AC}	12.7/12.7/12.7 [mm]
AC depth (Alberti, 2018)	ACD	3.45/4.35/5.00 [mm]
Posterior cornea minimum radius of curvature (Von Helmholtz, 1909)	R_C	6.8/6.8/6.8 [mm]
Radius of curvature of the natural lens	R_L	∞/∞/∞
Height of the iris–lens channel	–	0.24/0.24/0.24 [mm]
Angle between cornea and iris	–	45.8/55.1/69.5 [deg]
Aqueous humor		
Density (Spandau and Heinmann, 2012)	ρ	1000 [kg/m^3]
Kinematic viscosity	ν	$1.4 \cdot 10^{-4}$ [m^2/s]
Air		
Density (Spandau and Heinmann, 2012)	ρ	1.225 [kg/m^3]
Kinematic viscosity	ν	$1.4 \cdot 10^{-4}$ [m^2/s]
Surface tension with AH (Spandau and Heinmann, 2012)	σ_{air}	0.07 [N/m]
Iris contact angle	α_{iris}	20°
Lens contact angle (phakic) (Miyake et al., 1994)	α_{lens}	24°
Lens contact angle (pseudophakic)	α_{lens}	24°
Cornea contact angle (Alberti, 2018)	α_{cornea}	17°

of the ACD value, the patient's position and the time during the post-operative period, which is indirectly represented by the gas filling ratio, φ, i.e. the gas to total AC volume ratio, taking values between 0 and 1,

$$\varphi = \frac{V_{\text{gas}}}{V_{\text{AC}}}. \tag{1}$$

φ represents a non-dimensional time: immediately after surgery it attains a certain value; as time advances the eye progressively absorbs/evacuates the gas at a constant rate until no bubble is present, $\varphi = 0$. The actual time of evacuation is within 48 to 72 h after surgery (Tourtas et al., 2014).

The patient position is given by the gaze angle, ψ, see Fig. 1d, with −90° being the supine position; 0° horizontal gaze; and 90° the prone position. Usually, the gas volume in the AC after DMEK cannot be clinically measured. Therefore, two geometrical parameters were proposed in Pralits et al. (2019) to indirectly represent φ, namely two distances measured at $\psi = 0°$ from the topmost position of the AC: H_m, being the distance to the lower position of the gas bubble, and H_c, the distance to the lower position where the gas bubble touches the cornea. H_c can be obtained clinically using a slit-lamp while H_m is obtained from AS-OCT, both measured with the patient in horizontal position. In Fig. 2 values of H_c and H_m, non-dimensionalized with the AC diameter, as a function of ACD and gas filling ratio, for phakic and pseudophakic patients. These results are a generalization of those by Pralits et al. (2019).

2.3. The position of the bubble

The position of the gas bubble is evaluated by fitting an ellipse to the shape of the bubble interface projected on the cornea, see Fig. 3 for a phakic eye with an ACD = 3.68 mm, gas filling ratio of $\varphi = 0.68$ and gaze angle $\psi = 0°$. First the numerical results of the fluid–gas interface is transformed in gray scale, white being the interface. The fitting ellipse is described via its center $\mathbf{x_c}$ with respect to the AC center, its semi-major axis a and its eccentricity e. Here, the bubble move only in the vertical direction since patient motion is only described by the gaze angle, see Fig. 1d.

The shape and position of the gas bubble is not always intuitive. It depends on the equilibrium of forces due to gravity and surface tension. Moreover, it depends on the contact angles and the geometry of the anterior chamber, in particular the cornea. It is intuitive to think that the supine position always maximizes graft coverage. However, in Fig. 4 a counter example is given. There, a phakic geometry with ACD = 2.65 mm and $\varphi = 0.15$ is presented for two different patient positions: supine and horizontal gaze. The projection of the gas bubbles on the cornea for the two cases are shown along with the circumference of the graft. It is evident, that the case of horizontal gaze has a larger value of coverage, even though it is less centered compared to the supine case.

2.4. Recording of patient's position

Recording of the patient's position, in the patient-specific case, was performed as follows: A small inertial measurement unit (IMU)[1] was secured to the skin of the participant's temple with hydrocolloid dressing. A shielded wire from the IMU was connected to a waterproof plastic case hung on a string placed around the patient's neck. It contained a microcontroller,[2] a micro SD card data logger,[3] a button to aid the calibration process, a real-time clock[4] and a lithium-ion polymer battery[5] (3.7 V, 2500 mAh). Software features of the device included logging the values from the accelerometer, gyroscope, magnetometer, temperature and pressure sensor. Logging occurred twice per second, and each measurement was recorded with a date-time value from the real-time clock. Between each logging instance, sensor values were averaged from the 400 Hz measure rate. All patients were advised to lie in the face-up position for as much as possible for the first 72 postoperative hours.

[1] MPU-9250 accelerometer, gyroscope and magnetometer; Pesky Products, Danville, CA, USA.
[2] Teensy 3.2; PJRC, Portland, OR, USA.
[3] Teensy micro SD PJRC.
[4] DS3231 Precision RTC; Adafruit, New York, NY, USA.
[5] Adafruit.

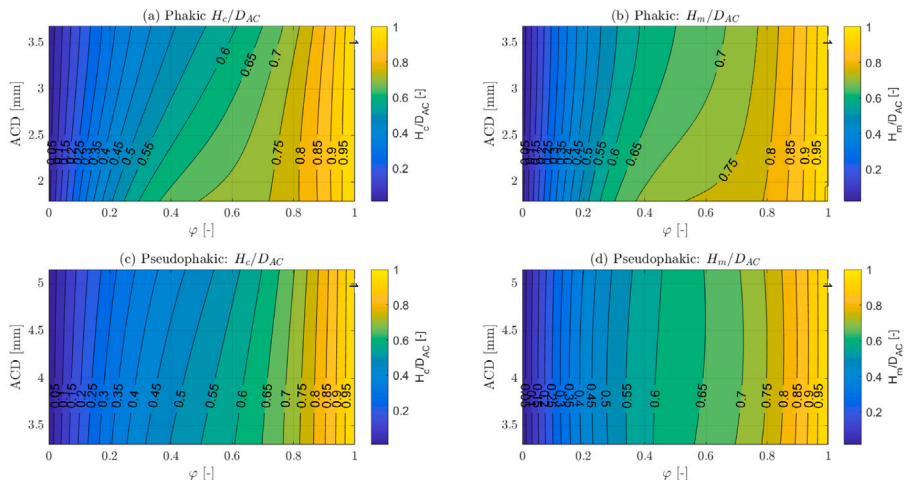

Fig. 2. Distribution of the values of H_c/D_{AC} and H_m/D_{AC} as a function of the gas filling ratio φ and the ACD for phakic (a,b) and pseudophakic (c,d) patients.

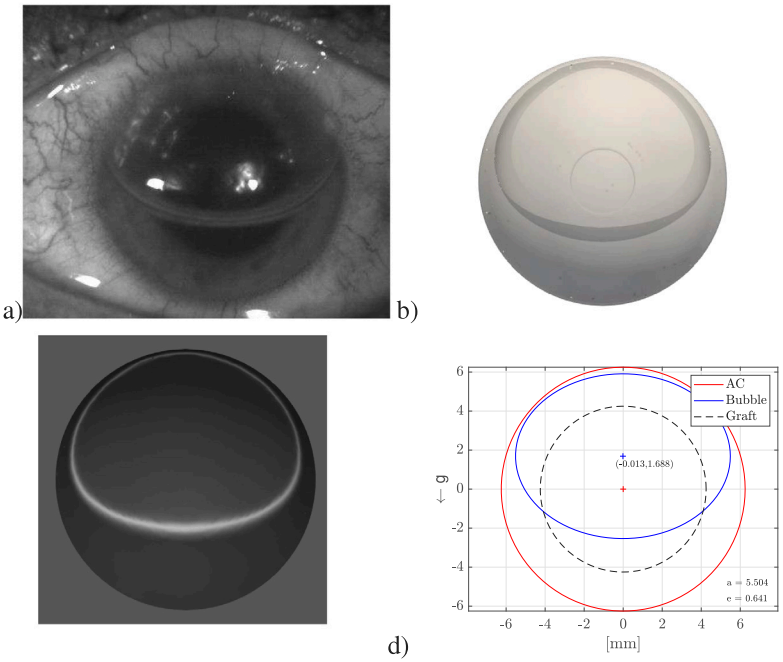

Fig. 3. Example of the ellipse detection method applied to a phakic patient with an ACD = 3.68 mm, a gas filling ratio of $\varphi = 0.68$ and gaze angle $\psi = 0°$. (a) Near infra-red image of a patient's eye after DMEK, (b) Numerical recreation of the patient's AC and its equilibrium state, (c) Gray-scale screenshot for ellipse detection, (d) Characteristic dimensions of the projection of the bubble on the cornea. (For interpretation of the references to color in this figure legend, the reader is referred to the web version of this article.)

3. Results

3.1. Description of the numerical experiments

The equilibrium position of the interface is investigated running simulations for different gas filling ratio, gaze angle and ACD. Each parameter is varied within a certain range: $\varphi \in [0, 1]$, $\psi \in [-90°, 90°]$, and the ACD values are given in Table 1. A total of 179 numerical simulations for phakic patients and 183 for pseudophakic ones are performed, using at least 5 values for each of the parameters φ and ψ.

3.2. Gas-graft coverage

The gas-graft coverage is measured as the percentage of graft surface in direct contact with gas, S_{gas}/S_{graft}. For phakic patients the gas-graft coverage is shown in Fig. 5a–b as a function of the gaze angle, ψ, and the gas filling ratio, φ. For small values of the ACD, the graft coverage is relatively symmetric around $\psi = 0°$, and the coverage is almost insensitive to the position of the patient. As the ACD increases, this symmetry is broken and the supine position of the patient gains importance. For example, a phakic patient with an ACD = 4 mm, see Fig. 5a–b, can experience differences of gas-coverage up to 35% depending on the orientation. In many cases, lying down face-up, $\psi = -90°$ is of most benefit and provides larger coverage. However, as shown in Fig. 4, in some cases other positions give larger coverage. Moreover, for $\varphi > 0.8$ the graft is nearly fully covered by the gas bubble at any gaze angle, independently of the value of the ACD.

Patients with an artificial lens tend to have larger ACD and volume compared to phakic patients, due to the flattening of the iris, see Fig. 1b. Then, the gas bubble moves more freely, making the position of the patient more important. As Fig. 5d shows, a pseudophakic eye with an ACD = 5.2 mm and $\varphi = 0.4$, can have half of the graft covered, down to no coverage, depending on the position. Unlike the phakic case, even

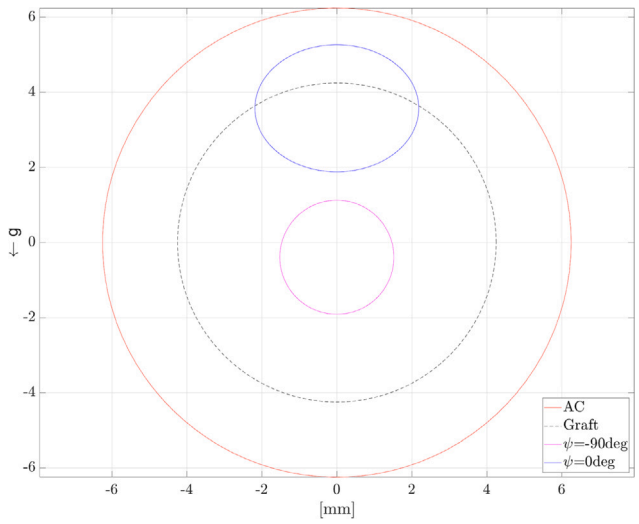

Fig. 4. The circumference of gas-graft coverage for two phakic cases: supine position and horizontal gaze. Here, the ACD = 2.65 mm and $\varphi = 0.15$.

narrow pseudophakic ACDs suffer up to 25% variation of the coverage depending on ψ.

3.3. Maximizing gas-graft coverage over time

The present data allows to determine the time history of the gaze angle which maximizes gas-graft coverage during the post-operative period. Its feasibility, considering the patients well being and therapeutic adherence, will be discussed in the next section. An example, for a phakic eye with ACD = 2.5 mm, is given in Fig. 6a. Time is represented through φ, whereas each red dot represents at a given time the gaze angle which maximizes the graft coverage. Only for certain times the best patient position is supine at $\psi = -90°$. Moreover, two intervals of gas fill have multiple solutions. For $\varphi > 0.8$ a complete coverage is obtained, independently of the value of gaze angle ψ. Finally, when $\varphi < 0.1$ the graft coverage is zero, independently of the value of gaze angle ψ..

In Fig. 6 the optimal time history of ψ is presented for different values of the ACD, both for phakic and pseudophakic eyes. As the ACD increases, the optimal position tends to be lying down facing up. As observed in Fig. 6b, pseudophakic patients with an ACD > 4.2 mm should be supine ($\psi = -90°$) during the whole post-DMEK period for maximum graft coverage. For large values of φ a range of optimal angles exist, see Fig. 6a. This range of gas filling ratios are not reported in Fig. 6 since they are rarely reached in the clinical case, and in order to make the interpretation of the intermediate values of φ more clear.

In Fig. 7a–b, the worst-case scenario is presented for both phakic and pseudophakic patients, where the gaze angle changes with time to yield the lowest gas-graft coverage. The black dots represent the case of random gaze angles. The theoretical maximum gas-graft coverage is essentially independent from the ACD and the lens' nature: provided the optimal gaze angle is maintained during the post-operative period, the graft will, on average, be covered by $60-65\%$. However, the minimum coverage decreases drastically as the ACD increases. Moreover, the difference between the maximum and minimum mean graft coverage becomes much larger as the ACD increases: around 2% for ACD = 1.5 mm and 25% for ACD = 4 mm. Unlike the phakic case, even smaller pseudophakic ACDs suffer large variations of the mean graft coverage if the position of the patient is not controlled, see Fig. 7b. This is even more critical for large ACDs: a pseudophakic patient with ACD = 5 mm has a maximum average coverage of 60% but a minimum of 35%.

3.4. Gas-graft coverage and therapeutic adherence

Not all optimal time histories are easy to realize: e.g. maintaining a precise angle $\psi = -53°$ for a long period is unpractical. Here we demonstrate that more comfortable and realistic positions do not significantly deteriorate gas-graft coverage compared to the optimal ones. Three different scenarios are presented in Fig. 7c–d: the theoretical maximum mean graft coverage, when the patient is always lying down facing up, when the patient is lying down facing up just after surgery (up to $\varphi = 0.5$) and then proceeds with random gaze angles. The optimal case and the one where the patient is always facing up are similar, although some difference arise in the phakic case. The difference becomes larger as the ACD increases. The sub-optimal alternatives seek to minimize discomfort and might increase the therapeutic adherence.

3.5. Coverage map

The occurrence of DMEK graft detachments motivates the need to also know the location and shape of the gas-graft contact. To this end we introduce the coverage map, i.e. a map that visualizes for how long every point of the graft has been covered by the gas bubble during the post-operative period, ranging from complete exposure to no exposure at all. The coverage map is obtained as follows: For each gas fill the shape, size and position of the gas bubble projected on the cornea are obtained. The coverage map is then obtained as the superposition of these results in time of the gas bubble at each point on the cornea.

Fig. 8a–c demonstrates the coverage map on a pseudophakic patient with ACD = 5 mm. The three scenarios (maximum, minimum and random graft coverage) are considered. In the worst-case scenario, not only the time-averaged graft coverage is low, but areas of the graft exist which are barely covered during the whole post-operative period. Moreover, the random gaze angle case yields a good mean coverage, only about 15% less than the maximum, but displays regions with an obvious deficit in contact. This again confirms that it is critical to provide the patient with a suggested position after DMEK. Maximum graft coverage is thus shown to imply a homogeneous contact distribution, whereas non-optimal situations lead to non-uniform coverage, and in particular are unable to cover the lower parts of the graft. This is critical since some investigations (Gorovoy, 2014) found that 82% of the occurrences of peripheral donor scrolls/contractions happened in the inferior quadrants. This discussion is less important when small phakic ACDs are considered. As Fig. 7 suggested, when the ACD decreases the difference between all the scenarios is at most of 5%. In addition (not shown here), small phakic ACDs tend to cover the graft area uniformly, thus monitoring the position of the patients becomes more critical as the AC volume increases, in particular for pseudophakic eyes.

3.6. Patient-specific coverage map

The coverage map method is also applied to a pseudophakic patient with an ACD = 3.76 mm, for which clinical data have been recorded, see Section 2. Fig. 9 shows the evolution of the gaze angle during the patient's post-operative period of 3 days, and the relative probability density function. The gaze-angle histogram shows that the patient's gaze angle was quite variable, but mostly being lying down facing up and down (consistent, for example, with sleeping). The dispersion around the $\pm 90°$ can be attributed to normal movements of the head.

Fig. 8d shows the computed patient-specific coverage map. The mean graft coverage is about 51%. As Fig. 7a–b shows, a pseudophakic patient with an ACD = 3.76 mm following a random gaze angle trajectory would have a mean graft coverage of around 53%. Thus, as the histogram suggested, it is safe to say that this patient did not undergo a strict monitoring of his/her position. The deficit compared to the maximum coverage is about 10%. What is more alarming, see Fig. 8d, is that this patient's trajectory led the gas bubble to fail covering the bottom quadrants, which might increase the possibilities of complications. In fact, adhesion problems in the inferior quadrant has already been observed in clinical trials (Tourtas et al., 2014).

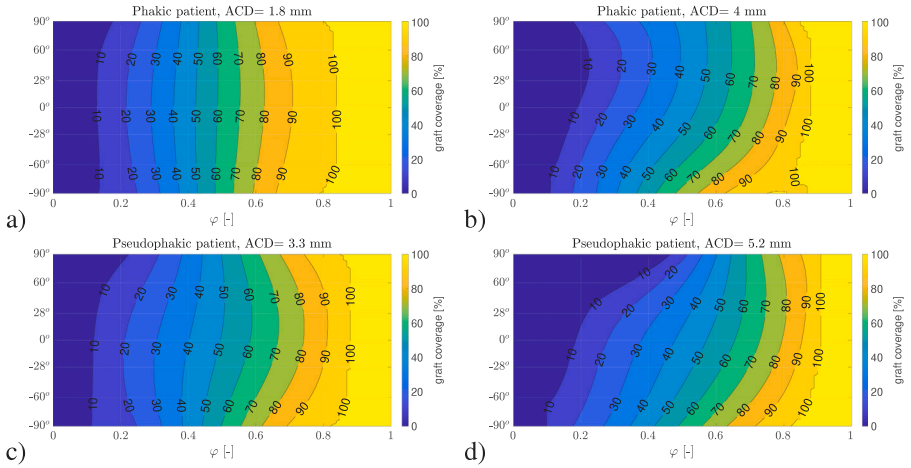

Fig. 5. Iso-contour curves in % of gas-graft coverage as a function of gas filling (φ) and gaze angle (ψ) in the case of: phakic patients and 2 different ACD values. (a) ACD = 1.8 mm, (b) ACD = 4.0 mm.: pseudophakic patients and 2 different ACD values. (c) ACD = 3.3 mm, (d) ACD = 5.2 mm.

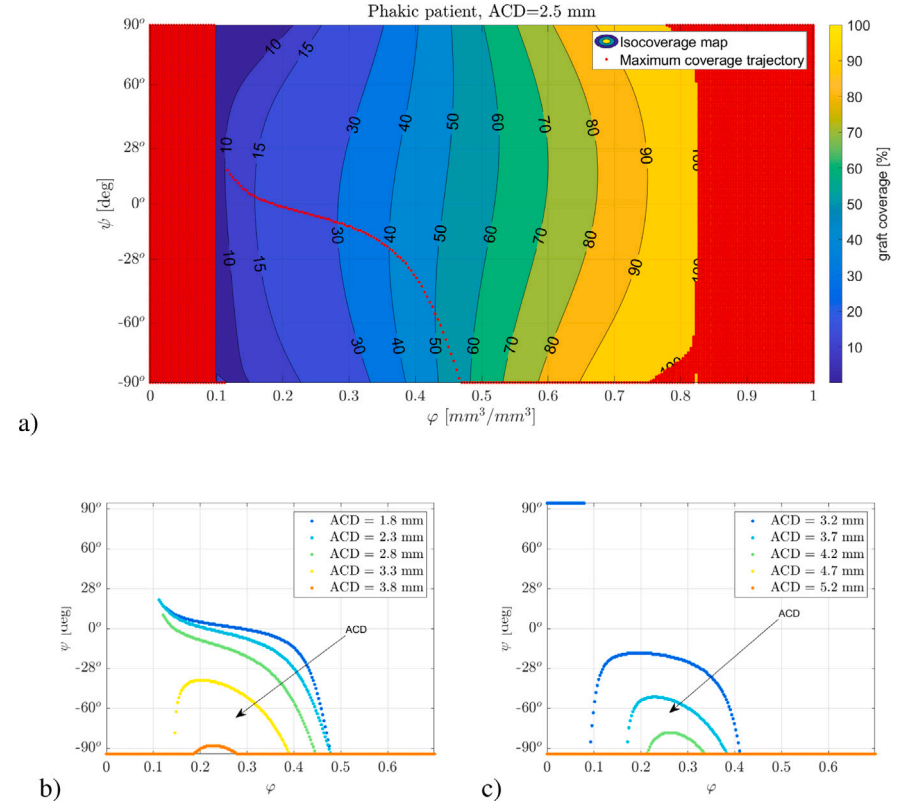

Fig. 6. Maximizing graft coverage: (a) Iso-contour curves in % of gas-graft coverage as a function of gas filling (φ) and gaze angle (ψ) in the case of phakic patients with ACD = 2.5 mm. For $\varphi > 0.8$ the red dots mark the maximum graft coverage, while for $\varphi < 0.1$ the red dots indicate zero graft coverage. Time history, for (b) phakic patients and (c) pseudophakic patients, of the gaze angle that maximizes gas-graft coverage, for various ACD. For $\varphi > 0.7$ wide ranges of gaze angle guarantee optimal coverage, see (a). (For interpretation of the references to color in this figure legend, the reader is referred to the web version of this article.)

4. Discussion

The gas bubble is critical for the success of DMEK surgery, but little is found in the literature about the exact behavior of the intraocular bubble in the post-operative period. Here, the shape, the size and the position of the bubble on the graft have been characterized in detail for phakic and pseudophakic patients, and for different values of the ACD, throughout the whole post-operative period. It has been shown that for small ACDs, especially in phakic eyes, the influence of the patients position on the graft coverage is minimal or negligible. A phakic eye with an ACD = 1.8 mm suffers variations of not more than ≈5% with respect to changes in ψ, see Fig. 5a–b. As the ACD increases the role of patient positioning gains dominance over the gas filling ratio. For example, a pseudophakic eye with an ACD = 5.2 mm and 40% gas fill can have 50% of the graft covered when lying down facing up but no coverage at all when facing down, see Fig. 5c–d. This same eye will also experience 50% variations on the graft coverage when decreasing the gas filling ratio to 10%, when the patient positioning is not optimal.

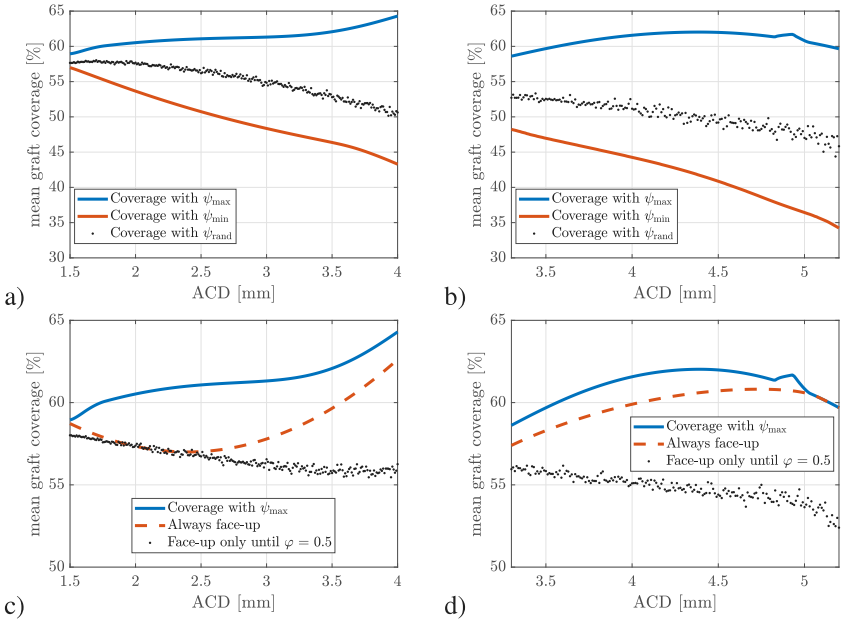

Fig. 7. (a,b) Mean graft coverage obtained by maximizing (ψ_{max}) and minimizing (ψ_{min}) w.r.t. the gaze angle. In addition, dots indicate a time history made by randomly-changing gaze angles (ψ_{rand}). (a) Phakic patients, (b) Pseudophakic patients. (c,d) Mean graft coverage obtained by maximizing (ψ_{max}) w.r.t. the gaze angle, mean graft coverage when the patient is always lying down face-up and the mean graft coverage when the patient is lying down face-up until $\varphi = 0.5$ and then proceeds to random gaze angles, (c) phakic patients, (d) pseudophakic patients.

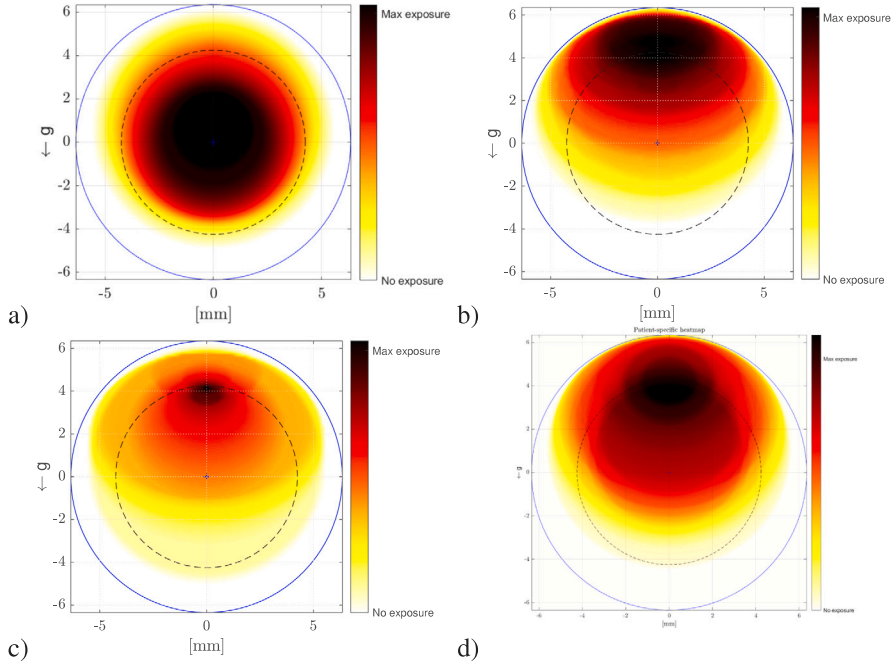

Fig. 8. (a,b,c) Coverage map for ACD = 5 mm for three different post-operative scenarios of pseudophakic eyes. (a) Maximum graft coverage trajectory (TAGC = 58.3%), (b) Random graft coverage trajectory (TAGC = 42.9%), (c) Minimum graft coverage trajectory (TAGC = 31.4%), (d) Patient-specific coverage map; pseudophakic eye with an ACD = 3.76 mm and the patients position given by Fig. 9 (TAGC = 51.4%). Here, TAGC denotes the Time-Averaged Graft Coverage.

However, with optimal positioning the decrease of graft coverage is only 10%. Thus, to monitor the patient's position carefully is more important for large ACDs compared to smaller ones.

When comparing best and worst-case scenarios, the difference of including or excluding variable gaze angles over time is minimal for small ACDs, especially in phakic cases. However, the differences become significant as the ACD increases, especially in pseudophakic eyes. For instance, when ACD = 5 mm the best/worst cases range from 60% to 35% time-average graft coverage during the post-operative period.

Complications after DMEK, such as graft detachment, justify the need of characterizing the position of the bubble as well. As the ACD increases, in particular in pseudophakic patients, the bubble tends to be in the superior half of the AC. This causes a coverage deficit in the lower half, see Fig. 8a–c. Hence, informing the patient about the correct positioning during healing, especially in the case of patients with large ACDs, is crucial to achieve both a high mean graft coverage and an evenly distributed gas-graft contact. Several of the maximum graft coverage trajectories given here are difficult to follow in practice,

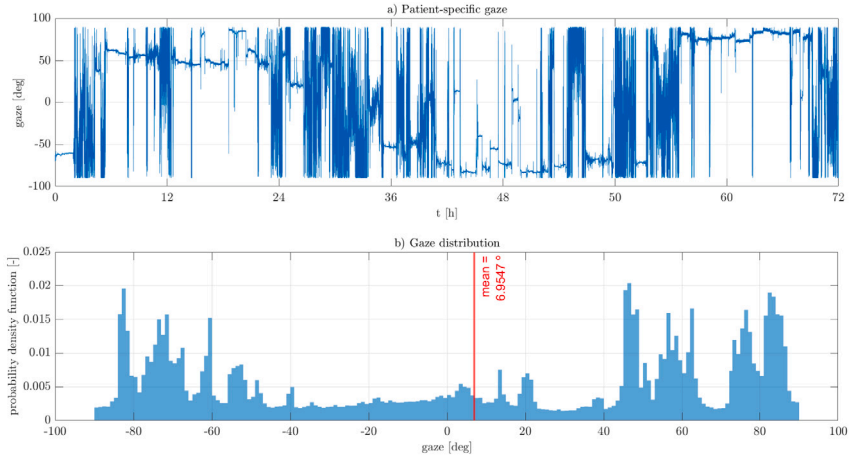

Fig. 9. (a) Patient-specific evolution of the gaze angle, (b) computed probability density function.

since they imply repeated changes of the patient's position. Therefore, suboptimal alternatives are proposed which are more practical to implement. In particular, since most patients are elderly, such alternatives seek to minimize discomfort. It is found that constantly being in the supine position is a good compromise between strictly following the required gaze angle and random changes without restrictions at all: it yields a homogeneous coverage with only 5% less mean coverage than the best-case scenario. The correlation between small ACD values and a possible decrease in post-surgical complications that could be attributed to less influence of patient position on graft coverage is currently being evaluated in Alberti (2018).

All the results discussed in this work are limited on different fronts. The geometries are simplifications of the real AC, and a rigid chamber has been considered instead of a flexible one with moving boundaries. After DMEK, drugs and the gas bubble affect the iris shape and, therefore, the shape of the AC. This is especially true in pseudophakic eyes, where extraction of the lens leaves ample room for iris mobility. Moreover, eye movements independent of the position of the patient have not been accounted for, Rossi et al. (2021) and Dvoriashyna et al. (2019). For example, during rapid eye movement sleep, sudden, fast, and random movements of the eye could imply displacements which were not recorded by the IMU on the patient's temple. The eye movements will invoke the motion of aqueous humor in the anterior chamber which inevitably will cause a motion, and alteration of the position, of the gas bubble and resulting graft coverage. Further, it is known that the healthy corneal endothelium actively pumps water towards the anterior chamber (Dvoriashyna et al., 2020; Cheng and Pinsky, 2017). It could be of interest to investigate its role in altering the bubble position and possibly the contact angle with the cornea in a future study.

CRediT authorship contribution statement

V. Garcia Bennett: Writing – original draft, Formal analysis, Data curation, Conceptualization. **M. Alberti:** Writing – original draft, Methodology, Formal analysis, Data curation. **M. Quadrio:** Writing – original draft, Supervision, Software, Resources, Project administration. **J.O. Pralits:** Writing – original draft, Supervision, Software, Project administration, Methodology, Conceptualization.

Declaration of competing interest

The authors declare that they have no known competing financial interests or personal relationships that could have appeared to influence the work reported in this paper.

Acknowledgments

The simulations were performed on resources provided by CINECA within the ISCRA C project HP10CYQL08.

References

Aiello, F., Gallo Afflitto, G., Ceccarelli, F., Cesareo, M., Nucci, C., 2022. Global prevalence of fuchs endothelial corneal dystrophy (FECD) in adult population: A systematic review and meta-analysis. J. Ophthalmol. 3091695. http://dx.doi.org/10.1155/2022/3091695.

Alberti, M., 2018. Air versus SF6 for descemet's membrane endothelial keratoplasty (DMEK), ClinicalTrials.gov NCT03407755. https://clinicaltrials.gov/ct2/show/NCT03407755.

Cheng, X., Pinsky, P.M., 2017. A numerical model for metabolism, metabolite transport and edema in the human cornea. Comput. Methods Appl. Mech. Engrg. 314, 323–344. http://dx.doi.org/10.1016/j.cma.2016.09.014, Special Issue on Biological Systems Dedicated to William S. Klug.

Ćirković, A., Beck, C., Weller, J., Kruse, F., Tourtas, T., 2016. Anterior chamber air bubble to achieve graft attachment after DMEK: Is bigger always better? Cornea 35 (4), 482–485. http://dx.doi.org/10.1097/ICO.0000000000000753.

Davvalo Khongar, P., Pralits, J.O., Cheng, X., Pinsky, P., Soleri, P., Repetto, R., 2019. A mathematical model of corneal metabolism in the presence of an iris-fixated phakic intraocular lens. Invest. Ophthalmol. Vis. Sci. 60 (6), 2311–2320. http://dx.doi.org/10.1167/iovs.19-26624.

Deng, S., Lee, W., Hammersmith, K., Kuo, A., Li, J., Shen, J., Weikert, M., Shtein, R., 2018. Descemet membrane endothelial keratoplasty: Safety and outcomes: A report by the American academy of ophthalmology. Ophthalmology 125 (2), 295–310. http://dx.doi.org/10.1016/j.ophtha.2017.08.015.

Dvoriashyna, M., Foss, A.J.E., Gaffney, E.A., Repetto, R., 2020. Fluid and solute transport across the retinal pigment epithelium: a theoretical model. J. R. Soc. Interface 17, 20190735. http://dx.doi.org/10.1098/rsif.2019.0735.

Dvoriashyna, M., Repetto, R., Tweedy, J.H., 2019. Oscillatory and steady streaming flow in the anterior chamber of the moving eye. J. Fluid Mech. 863, 904–926. http://dx.doi.org/10.1017/jfm.2018.889.

Gonzalez, A., Price, Jr., F., Price, M., Feng, M., 2016. Prevention and management of pupil block after descemet membrane endothelial keratoplasty. Cornea 35 (11), 1391–1395. http://dx.doi.org/10.1097/ICO.0000000000001015.

Gorovoy, M.S., 2014. DMEK complications. Cornea 33 (1), 101–104. http://dx.doi.org/10.1097/ico.0000000000000023.

Isakova, K., Pralits, J.O., Repetto, R., Romano, M.R., 2014. A model for the linear stability of the interface between aqueous humor and vitreous substitutes after vitreoretinal surgery. Phys. Fluids 26 (12), 124101. http://dx.doi.org/10.1063/1.4902163.

Isakova, K., Pralits, J.O., Romano, M.R., Beenakker, J.-W.M., Shamonin, D.P., Repetto, R., 2017. Equilibrium shape of the aqueous humor-vitreous substitute interface in vitrectomized eyes. Model. Artif. Intell. Ophthalmol. 1 (3), 31–46. http://dx.doi.org/10.35119/maio.v1i3.36.

Kopsachilis, N., Tsaousis, K., Tsinopoulos, I., Welge-Luessen, U., 2013. Air toxicity for primary human-cultured corneal endothelial cells: an in vitro model. Cornea 32 (4), e31–5. http://dx.doi.org/10.1097/ICO.0b013e31826895f8.

Landry, H., Aminian, A., Hoffart, L., Nada, O., Bensaoula, T., Proulx, S., Carrier, P., Germain, L., Brunette, I., 2011. Corneal endothelial toxicity of air and SF6. Invest. Ophthalmol. Vis. Sci. 52 (5), 2279–2286. http://dx.doi.org/10.1167/iovs.10-6187.

Leon, P., Parekh, M., Nahum, Y., Mimouni, M., Giannaccare, G., Sapigni, L., Ruzza, A., Busin, M., 2018. Factors associated with early graft detachment in primary descemet membrane endothelial keratoplasty. Am. J. Ophthalmol. 187, 117–124. http://dx.doi.org/10.1016/j.ajo.2017.12.014.

Melles, G., Ong, T., Ververs, B., van der Wees, J., 2006. Descemet membrane endothelial keratoplasty (DMEK). Cornea 25 (8), 987–990. http://dx.doi.org/10.1097/01.ico.0000248385.16896.34.

Miyake, K., Maekubo, K., Miyake, S., Yamauchi, A., Futamura, H., Gravagna, P., Tayot, J.L., 1994. Measuring contact angles of the lens capsule, collagen type I and collagen type IV. Eur. J. Implant Refract. Surg. 6 (3), 132–137. http://dx.doi.org/10.1016/S0955-3681(13)80403-0.

OpenFOAM, 2022. URL: https://www.openfoam.org.

Pralits, J.O., Alberti, M., Cabrerizo, J., 2019. Gas-graft coverage after DMEK: A clinically validated numeric study. Transl. Vis. Sci. Technol. 8 (6), http://dx.doi.org/10.1167/tvst.8.6.9.

Price, D.A., Kelley, M., Price, F.W., Price, M.O., 2018. Five-year graft survival of descemet membrane endothelial keratoplasty (EK) versus descemet stripping EK and the effect of donor sex matching. Ophthalmology 125 (10), 1508–1514. http://dx.doi.org/10.1016/j.ophtha.2018.03.050.

Repetto, R., Pralits, J.O., Siggers, J.H., Soleri, P., 2015. Phakic iris-fixated intraocular lens placement in the anterior chamber: Effects on aqueous flow. Invest. Ophthalmol. Vis. Sci. 56 (5), 3061–3068. http://dx.doi.org/10.1167/iovs.14-16118.

Rossi, T., Querzoli, G., Badas, M.G., Angius, F., Telani, S., Ripandelli, G., 2021. Computational fluid dynamics of intraocular silicone oil tamponade. Transl. Vis. Sci. Technol. 10 (8), 22. http://dx.doi.org/10.1167/tvst.10.8.22.

Spandau, U., Heinmann, H., 2012. Practical Handbook for Small-Gauge Vitrectomy. A Step-By-Step Introduction to Surgical Techniques, Vol. XIX. Springer.

Stuart, A.J., Romano, V., Virgili, G., Shortt, A.J., 2018. Descemet's membrane endothelial keratoplasty (DMEK) versus Descemet's stripping automated endothelial keratoplasty (DSAEK) for corneal endothelial failure. Cochrane Database Syst. Rev. 6 (6), CD012097. http://dx.doi.org/10.1002/14651858.CD012097.

Tourtas, T., Schlomberg, J., Wessel, J.M., Bachmann, B.O., Schlötzer-Schrehardt, U., Kruse, F.E., 2014. Graft adhesion in descemet membrane endothelial keratoplasty dependent on size of removal of host's descemet membrane. JAMA Ophthalmol. 132 (2), 155–161. http://dx.doi.org/10.1001/jamaophthalmol.2013.6222.

Von Helmholtz, H., 1909. Handbuch der Physiologischen Optik, third ed. University of Michigan Library.